

The Expected Inaccuracy in Measuring the Temperature Profiles in Solid Propellant by Thermocouple Elements

H. Milosevic^{1*}, A. D. Rychkov², N. Kontrec¹, and O. Taseiko³

¹Faculty of Science, University of Pristina in Kosovska Mitrovica,
Kosovska Mitrovica, Serbia

²Institute of Computational Technologies of Siberian Branch of
Russian Academy of Sciences, Novosibirsk, Russia

³Siberian State Aerospace University, Krasnoyarsk, Russia,
{mhrane, prof.a.d.rychkov, taseiko}@gmail.com, natasa_radenkovic@yahoo.com

Abstract. The behavior thermocouple in a solid medium is an interesting opportunity problem for accuracy of temperature measurement. This work considers interaction of thermocouple embedded in the solid substance pyrolyzed by external heat source with heat wave propagating inside the substance from the surface of its pyrolysis. Numerical simulation has shown that significant difference in the values of thermal conductivity coefficients of solid substance and thermocouple material results in the heat flow along thermocouple wires inside the substance that substantially changes thermo junction temperature thus misrepresenting thermocouple data.

Keywords: numerical simulation, heat transfer in solids, finite-difference methods, thermocouple measurement

1 Introduction

Subsurface thermocouple sensors are widely applied in various technical apparatus used for heat flux measurement in complex heat-stressed structures [1] and in various heat transfer devices [1] as well as at combustion of unitary solid fuels [2,3,4]. The evaluation of the consistency of values determined on the basis of thermocouple data becomes a problem. Errors result from the difference of thermophysical properties of thermocouple material and studied substance. At large temperature gradients in the heated substance, as a rule, heat outflow from the surface increases since thermal conductivity of metal thermocouples turns out to be substantially higher than thermal conductivity of the studied object substance. Extra difficulties are caused by variability of distance to the heat transfer surface conditioned by pyrolysis (carry-over) of the substance. In axisymmetrical statement, this problem was considered earlier in the work [5].

2 Mathematical Model Of Heat Wave Interaction With Thermocouple

Consider the process of temperature profile measurement in condensed substance pyrolyzed under the influence of external heat source. Formulate three-dimensional non-stationary problem of heat transfer between the solid and the embedded thermocouple (Fig. 1) assuming that substance pyrolysis rate and its surface temperature are constant. The thermocouple head is a sphere with radius R_m intersected at some angle 2α by two cylindrical conductors each with radius r_m . In this case, there are two planes of symmetry which allow reducing the size of the calculated area to a quarter from the full one. The view of solution area is shown in (Fig. 1a). Values of the angle α changed from 0 to 60°. It was assumed that at $\alpha = 0$ the wires were located so close to each other

* The work was financially supported by the Russian Foundation for Basic Research (Grant No. 09-01-12023of), and Project nr III 44006 financially supported by Ministry of Education, Science and Technology, Republic of Serbia, period 2010-2015.

that they could be replaced by one wire with double section area. In Cartesian coordinate system, this area is $D\{x_s(y, z, t) \leq x \leq x_{\max}, 0 \leq y \leq y_{\max}, 0 \leq z \leq z_{\max}, t \geq 0\}$, which external borders are selected at rather large distance from the thermocouple head to avoid the influence of heat transfer between the substance and the thermocouple on temperature distribution. Left boundary of the area is a plane surface of pyrolysis moving inside the substance with constant velocity r_b , and its position is determined by the correlation $x_s(y, z, t) = x_s(y, z, 0) + r_b t$. Coordinate origin is in the geometry center of the thermocouple spherical head. Equation of thermal conductivity in the area D is written in divergence form

$$\frac{\partial(\rho CT)}{\partial T} - \left(\frac{\partial}{\partial x} \left(\lambda \frac{\partial T}{\partial x} \right) + \frac{\partial}{\partial y} \left(\lambda \frac{\partial T}{\partial y} \right) + \frac{\partial}{\partial z} \left(\lambda \frac{\partial T}{\partial z} \right) \right) \quad (1)$$

where C , ρ and λ are specific heat capacity, density, and coefficient of heat conductivity.

These values are assumed constant but different in the areas occupied by the substance and thermocouple at which boundaries they change unevenly.

Recording of the equation (1) in divergence form provides correct calculation of heat fluxes in the case of discontinuous values of thermophysical parameters.

For equation (1), the following boundary conditions were set:

$$\begin{aligned} T(x_s, y, z, t) &= T_s; \\ \frac{\partial T(x, y, z, t)}{\partial x} \Big|_{x=x_{\max}} &= 0, \\ \frac{\partial T(x, y, z, t)}{\partial y} \Big|_{y=y_{\max}} &= \frac{\partial T(x, y, z, t)}{\partial y} \Big|_{y=y_0}, \\ \frac{\partial T(x, y, z, t)}{\partial z} \Big|_{z=z_{\max}} &= \frac{\partial T(x, y, z, t)}{\partial z} \Big|_{z=z_0} = 0. \end{aligned}$$

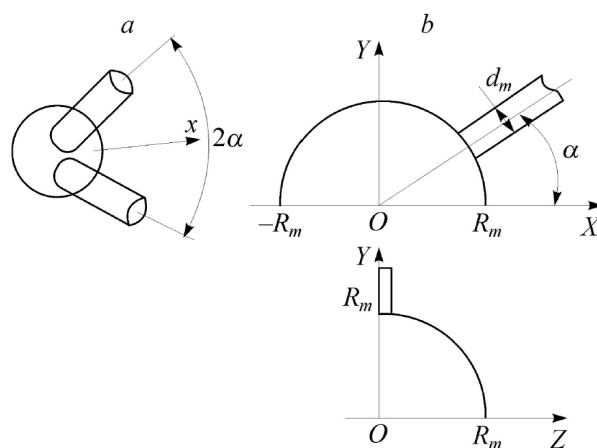


Fig. 1. Thermocouple arrangement scheme (a) and area of solution (b).

Initial conditions were set from the known Michelson solution describing temperature distribution in the plane heat wave moving along the OX axis with constant velocity r_b :

$$T(x, y, z, 0) = T_0 + (T_s - T_0) \exp(-r_b(x - x_s(0))C_p\rho_p/\lambda_p),$$

where index p relates to the substance parameters, T_s and T_0 are the pyrolysis temperature and initial temperature that were assumed constant. Initial position of the left boundary $x = x_s(0)$ is selected rather far from the thermocouple head top so that temperature distribution in thermocouple becomes close to T_0 .

3 Numerical Method Of Solution

For numerical solution of equation (1), the finite volume method was applied to carry out calculations on random finite-difference grid. The equation was written in in-tegral form for arbitrary fixed volume V :

$$\int_V \frac{\partial}{\partial t} Q dV + \oint_S \vec{\mathbf{F}} d\vec{\mathbf{S}} = 0, \quad (2)$$

where $Q = C\rho T$, $\vec{\mathbf{F}} = -\lambda\nabla T$ is heat flux through the normal-oriented element $d\vec{\mathbf{S}}$ of the surface S limiting the volume V . In the area D , let us build arbitrary difference grid with each cell topologically equivalent to parallelepiped. Designate the volume of such cell as $V_{i,j,k}$ and the average value Q on the n -th layer in time related to the center of such cell via $Q_{i,j,k}^n$. Then equation (2) is approximated by the following difference relation with the second order of accuracy in time and space:

$$\begin{aligned} & \frac{4Q_{i,j,k}^{n+1} - 3Q_{i,j,k}^n + Q_{i,j,k}^{n-1}}{2\tau} V_{i,j,k} + \left[(\vec{\mathbf{F}} \cdot \vec{\mathbf{S}})_{i+1/2}^{n+1} - (\vec{\mathbf{F}} \cdot \vec{\mathbf{S}})_{i-1/2}^{n+1} \right. \\ & \left. + (\vec{\mathbf{F}} \cdot \vec{\mathbf{S}})_{j+1/2}^{n+1} - (\vec{\mathbf{F}} \cdot \vec{\mathbf{S}})_{j-1/2}^{n+1} + (\vec{\mathbf{F}} \cdot \vec{\mathbf{S}})_{k+1/2}^{n+1} - (\vec{\mathbf{F}} \cdot \vec{\mathbf{S}})_{k-1/2}^{n+1} \right] = 0, \end{aligned} \quad (3)$$

where τ is the step in time. Scalar productions in square brackets are heat fluxes through respective areas of the volume facets $V_{i,j,k}$ multiplied by single normal to them. Method of their calculation is described in the work [6]. The obtained difference scheme is implicit, and for its solution we may apply the following iteration scheme based on the introduction of pseudo-time on each time layer in time:

$$\begin{aligned} & \left[\frac{Q_{i,j,k}^{n+1,s+1} - Q_{i,j,k}^{n+1,s}}{\tau_1} + \frac{4Q_{i,j,k}^{n+1} - 3Q_{i,j,k}^n + Q_{i,j,k}^{n-1}}{2\tau} \right] V_{i,j,k} \\ & + \left[(\vec{\mathbf{F}} \cdot \vec{\mathbf{S}})_{i+1/2}^{n+1,s} - (\vec{\mathbf{F}} \cdot \vec{\mathbf{S}})_{i-1/2}^{n+1,s} + (\vec{\mathbf{F}} \cdot \vec{\mathbf{S}})_{j+1/2}^{n+1,s} \right. \\ & \left. - (\vec{\mathbf{F}} \cdot \vec{\mathbf{S}})_{j-1/2}^{n+1,s} + (\vec{\mathbf{F}} \cdot \vec{\mathbf{S}})_{k+1/2}^{n+1,s} - (\vec{\mathbf{F}} \cdot \vec{\mathbf{S}})_{k-1/2}^{n+1,s} \right] = 0, \end{aligned} \quad (4)$$

where τ_1 is the step in pseudo-time and s is the number of iteration in pseudo-time. For realization (4), the scheme of splitting in spatial variables is used [7] (the subscripts are partially omitted):

$$\begin{aligned} & \frac{\delta^{s+1/3} - \delta^s}{\tau_1} V_{i,j,k} - \Lambda_1 \delta^{s+1/3} = \left[\frac{4Q_{i,j,k}^{n+1,s} - 3Q_{i,j,k}^n + Q_{i,j,k}^{n-1}}{2\tau} \right] V_{i,j,k} \\ & + \left[(\vec{\mathbf{F}} \cdot \vec{\mathbf{S}})_{i+1/2}^{n+1,s} - (\vec{\mathbf{F}} \cdot \vec{\mathbf{S}})_{i-1/2}^{n+1,s} + (\vec{\mathbf{F}} \cdot \vec{\mathbf{S}})_{j+1/2}^{n+1,s} - (\vec{\mathbf{F}} \cdot \vec{\mathbf{S}})_{j-1/2}^{n+1,s} \right. \\ & \quad \left. (\vec{\mathbf{F}} \cdot \vec{\mathbf{S}})_{k+1/2}^{n+1,s} - (\vec{\mathbf{F}} \cdot \vec{\mathbf{S}})_{k-1/2}^{n+1,s} \right], \quad (5) \\ & \frac{\delta^{s+2/3} - \delta^{s+1/3} \tau_1}{V_{i,j,k}} + \Lambda_2 \delta^{s+2/3} = 0, \\ & \frac{\delta^{s+1} - \delta^{s+2/3}}{\tau_1} V_{i,j,k} + \Lambda_3 \delta^{s+1} = 0, \quad Q^{n+1,s+1} = q^{n+1,s} + Q^{s+1}. \end{aligned}$$

Here δ^s are the corrections to the value Q ; A_1, A_2, A_3 are the difference operators considering only the second derivatives in respective directions. After iteration convergence on pseudo-time $\delta^s = 0$, exact approximation of complete initial equation takes place. The boundary conditions for δ^s are preset as follows. On the left boundary $\delta^s = 0$, on the other ones, "soft" boundary conditions are set. To calculate the value Q at the first step in time ($n = 0$) in the scheme (5), time approximation of the first order of accuracy was used since the values of the grid function $Q_{i,j,k}^{-1}$ are not known.

To build the curvilinear spatial difference grid we used the method based on numerical solution (scheme of stabilizing correction) of inverted two-dimensional Beltrami equations or diffusion in relation to the control metric [8]. The advantage of this method is possibility to build adaptive difference grids with preset properties. In particular, using the control metric we may control thickening of the grid nodes. This technology served to build the curvilinear block difference grid in the area D ; it thickened towards the area boundaries occupied by thermocouple. The grid was quasi-orthogonal in the vicinity of the section boundaries between the substance and the thermocouple. Such grid provided acceptable accuracy of calculations at small number of its nodes.

In the area between the left boundary and the thermocouple head, uneven rectangular difference grid was built that served to use the method of pyrolysis surface "trapping" in the grid node. The essence of the method is that the step in time was selected in such a way that at each further step in time, a position of the left boundary $x_s(t + \Delta t) = x_s(t) + r_b \Delta t$ coincided with the right closest vertical line of the difference grid. Then, a grid transformation during solution is not needed. Positions of the upper and right boundaries were selected to avoid significant effect on temperature distribution in the area occupied by thermocouple. The difference grid did not match the area boundaries occupied by thermocouple. Therefore, values of thermal conductivity coefficient at the cell boundaries were calculated as geometrical mean between its values at the centers of the adjacent cells. The values of $C \cdot \rho$ were calculated at the cell centers considering shares of these values for thermocouple and substance in the cell volume.

Accuracy of numerical solution was evaluated by calculations on progressively thickening grids. As a result, it was ascertained that the difference scheme with the number of grids in the area D $110 \times 110 \times 110$ over the coordinate axes provided relative accuracy of temperature calculations of approximately 0.1%.

4 Calculation Results

The calculations were performed for various radii of thermocouple head R_m , the wires' radii r_m were determined from the correlations $r_m/R_m = 0.2$ and 0.75 . The following values of thermophysical parameters were used:

$$\rho_p = 1.6[\text{g}/\text{cm}^3], \quad \rho_m = 8[\text{g}/\text{cm}^3], \quad C_p = 0.3[\text{cal}/(\text{g}\cdot\text{K})], \quad C_m = 0.2[\text{cal}/(\text{g}\cdot\text{K})], \quad \lambda_p = 0.00072[\text{cal}/(\text{cm}\cdot\text{s}\cdot\text{K})], \quad \lambda_m = 0.16[\text{cal}/(\text{cm}\cdot\text{s}\cdot\text{K})],$$

where index m stands for thermocouple material and index p for substance material. Temperature of pyrolysis surface $T_s = 650\text{K}$, initial temperature $T_0 = 300\text{K}$.

Calculations were carried out up to the moment of time when the pyrolysis surface contacted the thermocouple head. Values of thermocouple geometry parameters varied. Since spatial distribution of metal contacts forming thermocouple head and its voltage in seal is not clear we took the geometry center as a point for determination of thermocouple head temperature. Temperature at this point was determined by averaging over the volume of thermocouple head

V:

$$T_{av} = \iiint_V T(x, y, z, t) dx dy dz / \iiint_V dx dy dz.$$

The relative error of thermocouple temperature measurement was determined from the expression

$$\delta = \frac{T_\infty - T_{av}}{T_\infty} 100\%,$$

where $T_\infty = T(0, y_{\max}, z_{\max}, t)$ is the temperature at the point on the outer boundary of solution area rather remote from the thermocouple.

Two series of calculations were carried out, the first — at the pyrolysis rate $r_b = 0,1\text{cm/s}$, the second — at $r_b = 1\text{cm/s}$. Results of calculations are presented as dependence of relative error of temperature measurement $\delta(\xi)$ on dimensionless distance between pyrolysis surface and thermocouple head $\xi = R_m - x_s(t)/\Delta$, where $\Delta = \lambda_p/C_p\rho_p r_b$ is the width of the heat front of pyrolysis wave. Hatches designate variation of the relations of heat flux values from pyrolysis surface into solid

$$q = \left[\left(-\lambda_p \frac{\partial T}{\partial x} \right) \Big|_{\substack{x=x_s \\ y=0 \\ z=0}} \right] / \left[\left(-\lambda_p \frac{\partial T}{\partial x} \right) \Big|_{\substack{x=x_s \\ y=y_{\max} \\ z=z_{\max}}} \right]$$

at the points on symmetry axis and outer boundary. Width of heat front was $\Delta = 150\mu\text{m}$ at pyrolysis rate $r_b = 0.1\text{cm/s}$ and $\Delta = 15\mu\text{m}$ — at $r_b = 1\text{cm/s}$, respectively. Behavior of the $\delta(\xi)$ value at $r_b = 0.1\text{cm/s}$ is shown in (Fig. 2, 3, 4, 5). It is seen that wire configuration determined by the angle α significantly influences the value of the measurement error. The least measurement error is provided by the thermocouple with the least head radius. Presence of maximum on the curves is bound with the fact that when the pyrolysis front approaches the thermocouple head the heat outflow over the wires inside the solid substance increases, however, further at small distances ξ the thermocouple head heating sharply increases that results in the decrease of the value $\delta(\xi)$.

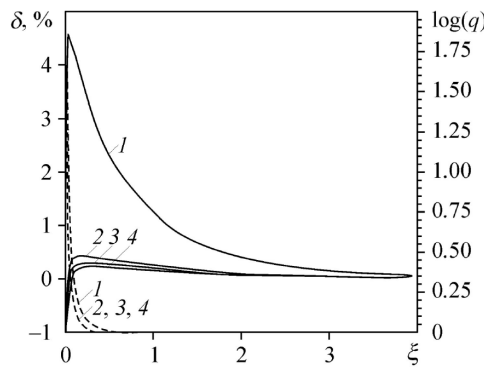


Fig. 2. Variation of $\delta(\xi)$ for $R_m = 12\mu\text{m}$ ($r_m/R_m = 0.2$). ≡Figure 6 $\alpha = 0^\circ$ (1), 15° (2), 45° (3), 60° (4).

In (Fig. 6, 7, 8, 9) there are results of analogous calculations at pyrolysis rate $r_b = 1\text{cm/s}$. It is seen that along with the increase in a thermocouple head radius the measurement error decreases, and at $R_m > 40\mu\text{m}$ it even becomes negative. This is bound with the fact that at larger dimensions of thermocouple head, the width of the heat wave becomes lesser than the head

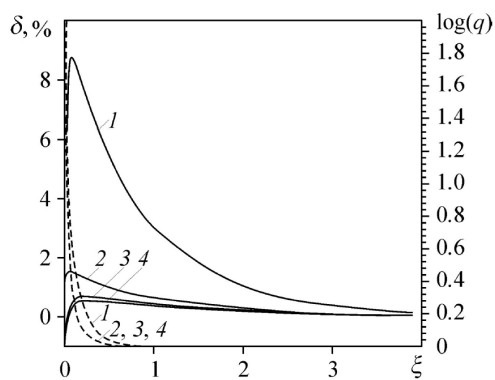


Fig. 3. Variation of $\delta(\xi)$ for $R_m = 20\mu m$ ($r_m/R_m = 0.2$). \equiv Figure 7 $\alpha = 0^\circ$ (1), 15° (2), 45° (3), 60° (4).

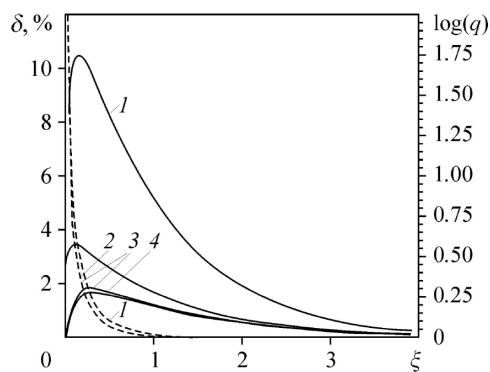


Fig. 4. Variation of $\delta(\xi)$ for $R_m = 45\mu m$ ($r_m/R_m = 0.2$). \equiv Figure 8 $\alpha = 0^\circ$ (1), 15° (2), 45° (3), 60° (4).

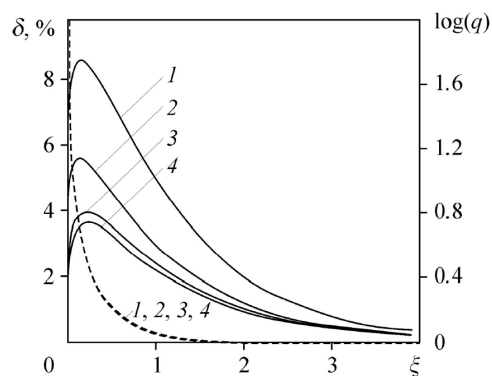


Fig. 5. Variation of $\delta(\xi)$ for $R_m = 120\mu m$ ($r_m/R_m = 0.2$). \equiv Figure 9 $\alpha = 0^\circ$ (1), 15° (2), 45° (3), 60° (4).

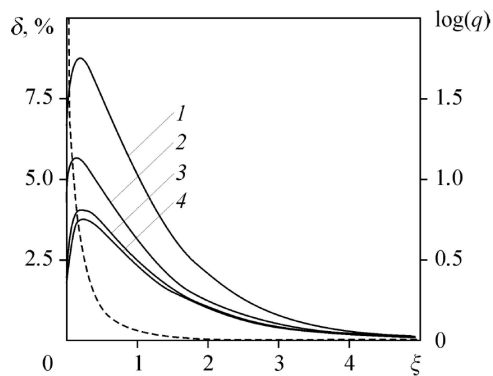


Fig. 6. Variation of $\delta(\xi)$ for $R_m = 12\mu m$ ($r_m/R_m = 0.2$). \equiv Figure 2 $\alpha = 0^\circ$ (1), 15° (2), 45° (3), 60° (4).

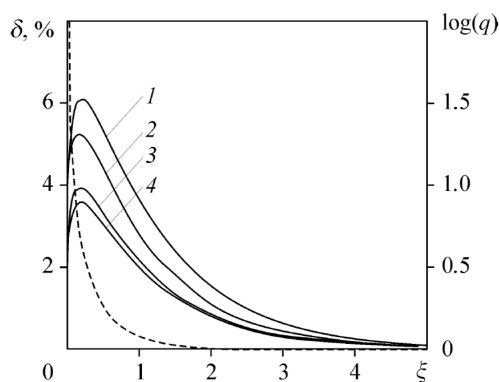


Fig. 7. Variation of $\delta(\xi)$ for $R_m = 20\mu m$ ($r_m/R_m = 0.2$). \equiv Figure 3 $\alpha = 0^\circ$ (1), 15° (2), 45° (3), 60° (4).

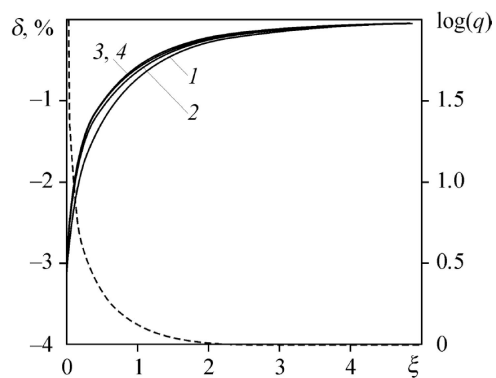


Fig. 8. Variation of $\delta(\xi)$ for $R_m = 45\mu m$ ($r_m/R_m = 0.2$). \equiv Figure 4 $\alpha = 0^\circ$ (1), 15° (2), 45° (3), 60° (4).

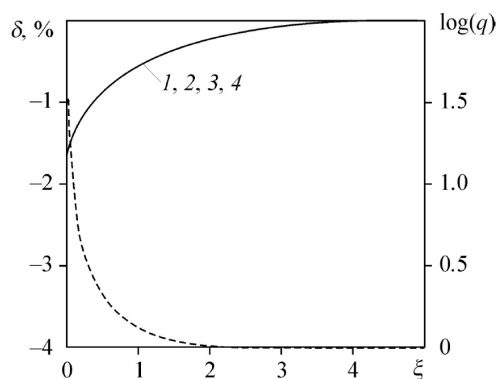


Fig. 9. Variation of $\delta(\xi)$ for $R_m = 120\mu\text{m}$ ($r_m/R_m = 0.2$). \equiv Figure 5 $\alpha = 0^\circ$ (1), 15° (2), 45° (3), 60° (4).

diameter. Therefore, in this case the head simply has insufficient time for heating that influences the error value.

Absolutely analogous behavior of the value δ shown in (Fig. 10), takes place at small pyrolysis rate for rather large dimensions of thermocouple head as well. For thermocouples with relatively large radii of wires with correlation $r_m/R_m = 0.75$, the measurement error turns out to be much higher (Fig. 11), that is bound with the increase in heat flux in the wires because of the increase in the areas of their transverse sections.

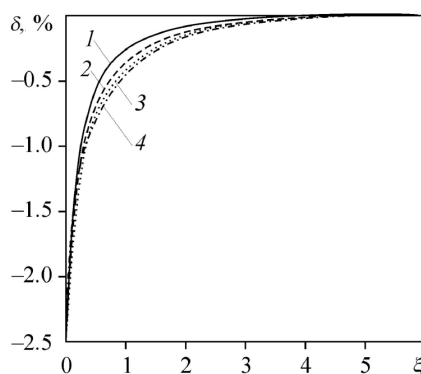


Fig. 10. Variation of $\delta(\xi)$ for $R_m = 400\mu\text{m}$ ($r_b = 0.1\text{cm}$, $r_m/R_m = 0.2$). $\alpha = 0^\circ$ (1), 15° (2), 45° (3), 60° (4).

The obtained results prove that accuracy of information on temperature distribution in near-surface layer of solid substance which thickness is comparable with the front width of pyrolysis hear-wave may be rather unreliable. Moreover, heat sink into thermocouple results in significant increase of heat outflow from pyrolysis surface at its approaching a thermocouple that may result in significant change of pyrolysis rate in the vicinity of thermocouple head. Values $q(\alpha)$ in the moment of pyrolysis surface approach to thermocouple head are given in the table for two rates of pyrolysis. It is seen that the behavior of this value at the increase of the angle α significantly depends on thermocouple head size and pyrolysis rate determinant for heat overflows between the head and wires. This fact may serve an additional source for inaccuracy at thermocouple temperature measurement in the near-surface layer.

5 Conclusions

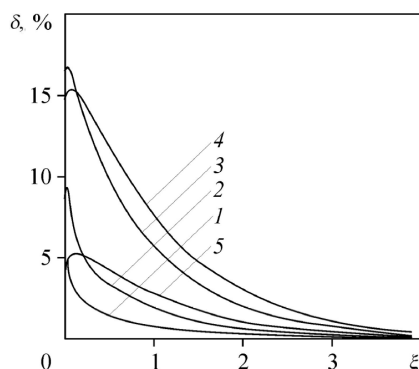


Fig. 11. Variation of $\delta(\xi)$ for $r_m/R_m = 120\mu\text{m}$ ($r_b = 0.1\text{cm/s}$, $\alpha = 60^\circ$). $\alpha = 0^\circ$ (1), 15° (2), 45° (3), 60° (4).

Table 1. Dependencies of heat flux values on the angle α

$R_m \mu\text{m}$	$r_b = 0.1\text{cm/s}$				$r_b = 1.0\text{cm/s}$			
	0°	15°	45°	60°	0°	15°	45°	60°
12	53.4	23.8	19.8	19.8	123.8	120.7	131.8	145.3
20	94.4	56.6	44.3	43.9	91.0	105.2	121.7	137.7
45	137.5	110.9	101.8	105.7	59.8	61.5	73.2	84.1
120	128.8	125.8	138.6	153.9	27.4	28.2	33.8	40.0
400	64.2	66.0	77.7	88.4				

1. Numerical simulation has revealed significant error at thermocouple temperature measurement in solid at its pyrolysis, and the error value depends both on pyrolysis rate and geometry dimensions of thermocouple.
2. The obtained results may be used to correct the error of temperature measurement with the use of thermocouples at experimental investigations of solids pyrolysis.

References

1. T. V. Borovkova, Y. N. Yeliseyev, and I. I. Lopukhov, *Mathematical modeling of contact thermo-couple*, Physics of Particles and Nuclei Letters, **5**(3), 274–277 (2008).
2. G. A. Franco, E. Caron, and M. A. Wells, *Quantification of the surface temperature discrepancy caused by surface thermocouples and methods for compensation*, Metallurgical and Materials Transactions B, **338B**, 949–956 (2007).
3. A. A. Zenin, *Errors of thermocouple measurements of flames*, J. Engng. Phys., **5**(5), 67–74 (1962).
4. A. A. Zenin, *Heat transfer of thermocouples in solid fuel combustion waves*, J. Appl. Mech. and Techn. Phys., **5**, 125–131 (1963).
5. B. W. Asay, S. F. Son, P. M. Dickson, L. B. Smilowitz, and B. F. Henson, *An investigation of the dynamic response of thermocouples in inert and reacted condensed phase energetic materials*, Pro-pellants, Explosives, Pyrotechnics, **30**(3), 199–208 (2005).
6. A. D. Rychkov, L. K. Gusachenko, and V. E. Zarko, *Accuracy estimation of thermocouple temperature measurement in solid fuel*, Papers of VI Meeting of Rus.-Kazakh Work Group in Comp. and Inform. Technol., Kazakh National University, Almaty, 282–286 (2009).
7. M. Vinokur, *An analysis of finite-difference and finite-volume formulations of conservation laws*, J. Comput. Phys., **81**, 1–52 (1989).
8. N. N. Yanenko, *Fractional Step Method for Solving Problems of Mathematical Physics*, Nauka, Novosibirsk 1967.
9. V. D. Liseikin, *A Computational Differential Geometry Approach to Grid Generation*, second edition, Springer, Berlin, 2007.